2015

Comparing segmented ASL perfusion of vascular territories using manual versus semiautomated techniques in children with sickle cell anemia

K. J. Helton

J. O. Glass

W. E. Reddick

A. Paydar

A. R. Zandieh

See next page for additional authors

HHS Public Access

Author manuscript

J Magn Reson Imaging. Author manuscript; available in PMC 2016 February 01.

Published in final edited form as:

J Magn Reson Imaging. 2015 February ; 41(2): 439–446. doi:10.1002/jmri.24559.

Comparing segmented ASL perfusion of vascular territories using manual vs. semi-automated techniques in children with sickle cell anemia

Kathleen J. Helton, M.D.[1], **John O. Glass, M.S.**[1], **Wilburn E. Reddick, Ph.D.**[1], **Amir Paydar, M.D.**[1], **Arash R. Zandieh, M.D.**[1], **Rachna Dave, B.S.**[1], **Matthew P. Smeltzer, M.S.**[2], **Song Wu, Ph.D.**[2], **Jane Hankins, M.D.**[3], **Banu Aygun, M.D.**[3], and **Robert J. Ogg, Ph.D.**[1]

[1]Department of Radiological Sciences, St Jude Children's Research Hospital, Memphis, TN

[2]Department of Biostatistics, St Jude Children's Research Hospital, Memphis, TN

[3]Department of Hematology, St Jude Children's Research Hospital, Memphis, TN

Abstract

Purpose—Elevated cerebral blood flow (CBF) in sickle cell anemia (SCA) is an adaptive pathophysiologic response associated with decreased vascular reserve and increased risk for ischemia. We compared manual (M) and semi-automated (SA) vascular territory delineation to facilitate standardized evaluation of CBF in children with SCA.

Materials and Methods—ASL perfusion values from 21 children were compared for gray matter and white matter (WM) in vascular territories defined by M and SA delineation. SA delineated CBF was compared with clinical and hematologic variables acquired within 4 weeks of the MRI.

Results—CBF measurements from M (MCA 82 left, 79 right) and SA (MCA 81 left, 81 right) delineated territories were highly correlated (R=0.99, $p < .0001$). Bland-Altman plots had close-fitting limits of agreement of −1.8 to −3.5 lower limit and 0 to 1.8 upper limit. SA vascular territory delineation was comparable to the expert delineation with a kappa index of 0.62–0.85 and was considerably faster. Median territorial CBF values did not differ by gender or age. WM perfusion in the posterior cerebral artery territories was positively correlated with degree of hemolysis (R=0.58, p=.01 left, 0.73, p<.001 right) and negatively correlated with hemoglobin (R= −0.48, p=.03 left, −0.47, p=.04 right) and hemoglobin F (R=−0.42, p=.09 left, −0.47, p=.049 right).

Conclusion—We established the validity of the SA method, which in our experience was much faster than the M method for delineation of vascular territories. Associations between CBF and hematologic variables may demonstrate pathophysiologic changes that contribute to clinical variation in CBF.

Correspondence: Correspondence to: Kathleen J. Helton, M.D., Department of Radiological Sciences, St. Jude Children's Research Hospital, 262 Danny Thomas Place, MS 220, Memphis, TN 38105-3678, Phone: (901) 595-3827, FAX: (901) 595-3981, kathleen.helton@stjude.org.

Keywords

semi-automated perfusion; sickle cell anemia; ASL

Introduction

While enormous progress has been made in our understanding of sickle cell anemia (SCA), much work still needs to be done to impact the complex morbidity and mortality of this disease (1). Clinical trials have characterized the spectrum of brain injury; the incidence of clinical stroke approaches 11% by 20 years of age, the incidence of silent infarction ranges from 17–35%, and severe neurological and neurocognitive injuries are not uncommon (2, 3). While the average life expectancy for a patient with SCA in the United States was only in the mid-40s in 1994 (4), with early and more comprehensive treatment, the childhood life expectancy continues to increase (5). But as demonstrated by Vinchinsky et al, clinically normal adults with SCA had significantly poorer performance compared with normal controls on measures of global IQ, cognitive function, working memory, processing speed and executive function, which were related to both age and anemia (6). The need for monitoring the future success of early childhood interventions in SCA may in part be met by advanced imaging techniques.

Recent imaging studies, often using arterial spin labeling (ASL), have explored the hyperemic adaptive responses to chronic anemia (7–11). While the adaptive response of elevated cerebral blood flow (CBF) initially optimizes tissue oxygenation, the maximized flow rates limit further perfusion adaptation, contribute to large and small vessel injury/ischemia, and neurocognitive impairment. (7–9, 11–15). Unfortunately there is no standardized approach to quantification, segmentation of gray matter (GM) from white matter (WM), or a uniform approach to delineation of vascular territories (7–11), which makes comparison among different studies difficult. Furthermore, in our experience, manual delineation of vascular territories is very time consuming. Standardized and efficient methods for vascular territory-based evaluation of CBF are needed for prospective trials, to assess the impact of therapies on CBF and to correlate these findings with other clinical parameters longitudinally.

In this paper we report a semi-automated (SA) method for delineation of the major vascular territories in the human brain, and use it in conjunction with tissue segmentation (16) to characterize patterns of CBF in a cohort of SCA subjects. The difference in CBF measured with the SA method was compared to that of the manual (M) method using Pearson Correlation Coefficients and Bland Altman Plots. After establishing the validity of the SA method, we explored the association of CBF with hematological variables.

Methods

Patient Selection

The study included 21 children with SCA (median age 12 years, range 5–17, M = 15, F= 6, M: F ratio 2.5) who were enrolled after informed consent on an IRB-approved prospective

imaging study exploring the feasibility of diffusion tensor imaging, ASL perfusion and functional MRI (11). Although prospective in nature, the convenience sample (non-randomized subjects willing to participate from the Hematologic Clinic) enrolled 18 of 21 children who had been on hydroxyurea therapy. No participant had a prior history of a clinical stroke, had received a transfusion within the past 30 days, or required sedation for their MRI exam.

MR Imaging Studies

All participants underwent ASL perfusion imaging and conventional MR imaging (cMRI) with a 1.5-Tesla scanner (Siemens Medical Systems, Iselin, NJ). Imaging parameters were as follows: T1-weighted (TR/TE=552/9 msec), proton density (PD) and T2-weighted (TR/TE1/TE2=4470/16/109 msec), fluid attenuated inversion recovery (FLAIR) (TR/TE/TI=9140/112/2400 msec), and pulsed ASL Q2TIPS (16) (TR/TE=2200/13 msec, TI=700 msec, TIS=1400 msec, 64×64 matrix, 256 mm FOV, 5 mm thick with 2.5 mm gap, and 1 average) which was available as a work-in-progress package from Siemens Medical Systems. All T1, T2, and PD images were acquired to ensure complete head coverage and included 27 slices (5 mm thick) without gap and a 256×256 matrix. Conventional T1, T2, and PD images were co-registered to ASL images for manual delineation of 12 vascular territories based on Tatu's accepted regional vascular atlas (17), as well as segmentation into 4 tissue classifications, GM, WM, cerebral spinal fluid (CSF) and leukoencephalopathy (LE) (11). For this segmentation process, the MRI sets within an individual examination were registered, intensity inhomogeneity corrected (18), and tissues were segmented using an automated hybrid neural network segmentation and classification method (19). Considerable reliability and validity have been established for these methods, resulting in a predicted variance of approximately two percent in the repeated measure of white and gray matter (20).

Semi-Automated Vascular Territories

A semi-automated method was developed in which vascular territories were defined based on the review of several accepted vascular atlases (21–25), consolidated into consistent conventional regions. This technique relied on identifying anatomic landmarks and assigning pre-determined vascular territory divisions in an atlas space based on their relation to these landmarks. These landmarks were identified by experienced imaging scientists (JOG, 19 years experience) under the direct supervision of the principal investigator (KJH, 15 years experience). Initially, an individual subject's T2-weighted image was registered to the ICBM T2-atlas in Talarach space using normalized mutual information. This T2-weighted image was then masked to remove both the extra-meningeal tissues and posterior fossa. The semi-automated technique relied on identifying anatomic landmarks on three specific sections: 1) at the level the ventricles first appear, 2) the level of the basal ganglia at the lowest point of the genu of the corpus callosum [CC], and 3) at the most inferior extent of the genu of the CC, at the level of the thalamus and first appearance of the cerebellum. Details of the anatomical landmarks selected at each of these levels is detailed and demonstrated in Figure 1. These landmarks were then used in the semi-automated technique to assign pre-determined vascular territory divisions in the atlas space to distinguish the left and right anterior cerebral artery (ACA), middle cerebral artery (MCA), and posterior

cerebral artery (PCA) regions as shown in Figure 2. An attempt was made to exclude the expected distribution of the anterior choroidal artery. The process of combining the segmentation of GM and WM, the identification of the vascular territories, and the pulling of data from the ASL output map is demonstrated in Figure 3.

Comparison of Manual and Semi-Automated Vascular Territories

The semi-automated delineated vascular territories were output into a gray scale image format. This image was then registered to the individual subject's ASL space where the manual territories were delimited. Registered semi-automated vascular territory maps were then manually verified to reside in the proper hemisphere and converted into the same file format as the manual regions to facilitate comparisons. Comparison of manual vs. semi-automated analysis of gray and white matter CBF by whole brain, hemisphere and vascular territory was performed (Figure 2). Beyond a qualitative comparison of the two techniques as shown in this figure, overlap of the regions was assessed with Kappa statistics, correlations between the resulting CBF values were calculated, and differences in the CBF values were plotted. The details are contained in the following statistical analysis section. We observed the time requirements for delineation by the M vs the SA technique. Additionally, we investigated the associations of semi-automated delineated CBF with clinical (age, gender, number of hospitalizations for acute chest syndrome episodes (26)) and hematologic variables (white blood cell count count [WBC], total bilirubin, absolute reticulocyte count [ARC], hemoglobin [Hb] and hemoglobin F [HbF]), acquired within 4 weeks of the MRI.

Statistical Analyses

Correlations between continuous variables were assessed using the Pearson Correlation Coefficient and the associated p-values. Due to the low number of females, median CBF values were compared between genders with the nonparametric Wilcoxon Mann Whitney test (27). Agreement between CBF in the manual vs. semi-automated methods was assessed using Bland-Altman plots (28) and limits of agreement. Limits of agreement provide an estimate for the amount of variation that could be expected when interchanging the two methods. The Kappa Index (KI) of similarity was used to measure the agreement of the pixels selected by the manual and semi-automated methods. According to Landis, an almost perfect agreement occurs if the KI value equals 0.81–1.00 and is substantial for values of 0.61–0.80 (29). P-values less than 0.05 were considered statistically significant and no adjustments were made for multiple comparisons due to the exploratory nature of this study.

Results

Comparison of manual vs. semi-automated delineation of vascular territories

Historically we observed that the delineation by the M method took four to five hours per patient. In contrast, the SA method took approximately ten minutes to remove cerebellum from the data set, five minutes to identify and input the landmarks, and only one minute to run the semi-automated program. The CBF values using the SA and M techniques are demonstrated in Table 1. We first analyzed the correlations between the CBF of GM and WM by whole brain, hemispheres and all six vascular territories (bilateral anterior, middle

and posterior cerebral artery) and found predominantly very strong correlations between CBF measured by manual delineation versus the semi-automated method (Table 2). Bland-Altman plots and limits of agreement were used to assess the level of agreement between the manual delineation versus the semi-automated method for each region. The agreement varied over the regions examined. The plots comparing the manual vs. semi-automated delineation by whole brain and hemisphere showed excellent agreement and close-fitting limits of agreement for both GM and WM (Figure 4). The strongest regional agreements were for the bilateral middle cerebral artery territories (GM R=0.99 left, R=0.99 right; WM R=0.98 left, R=0.98 right) (Table 2), with small bias and close-fitting limits of agreement. Additionally, the Kappa Index showed substantial (ACAs, PCAs) to almost perfect agreement (MCAs) between the pixels selected by both techniques (Left/Right Anterior, Posterior, and Middle Cerebral Arteries [KI 0.67/0.68, 0.65/0.62, 0.82/0.85] (29).

Associations with clinical and demographic variables

Only hematological variables acquired within 30 days of the MRI were examined. The variables were acquired within a median of 3 days (0–19) for the Hb and WBC count, a median of 8 days (0–28) for the HbF and a median of 4.5 days (0–21) for the ARC of the MRI examination. The WBC count and number of lifetime acute chest syndrome episodes were not associated with CBF. The hematologic variable Hb showed a statistically significant negative correlation with WM CBF in the bilateral PCA territories. HbF showed a statistically significant negative correlation with WM CBF in the right PCA territory, and a negative trend in the left PCA territory. The ARC showed a statistically significant positive correlation with WM CBF in the whole brain, bilateral hemispheres and the bilateral PCA, and right MCA territories (Table 3). The GM CBF also showed a statistically significant positive correlation with ARC in the bilateral PCA territories. Additionally, WM CBF in the left MCA territory showed a positive trending correlation to the ARC. The median values of these hematological variables, more closely matching normal population values as opposed to those with SCD (11), likely reflected prior treatment with HU in the majority (18 of 21) of the subjects (Table 4). Although our cohort had a male to female ratio of 2.5, there were no gender differences in any of the perfusion comparisons. Similarly, no significant associations between age and perfusion were detected.

Discussion

Sickle cell anemia is an autosomal recessive hemolytic anemia characterized intracranially by large and small vessel vasculopathy, with adaptive elevated cerebral blood flow and vasodilatation (3, 11, 14). Although SCA remains the most frequent etiology of clinical stroke and silent infarct in children, the pathophysiology of these phenomena is complex (15, 30). Because of the broad range of brain pathology related to the altered cerebral hemodynamics in patients with SCA, there is a need for a standardized, time efficient way, to quantify these changes. Our study demonstrated that the semi-automated method reliably identified major cerebral vascular territories that were consistent with those identified manually. The mean territorial CBF values determined by the two methods were highly correlated. Furthermore, the semi-automated method may reduce operator-dependent bias,

and will facilitate prospective longitudinal research, to better characterize the effects of treatment on regional GM and WM CBF.

Quantification of CBF was previously performed by intravenous administration or inhalation of radionuclide (12, 31, 32) or intravenous injection of MRI contrast (33). With the advent of ASL perfusion techniques, which measure labeled arterial protons at the capillary level, it has become possible to non-invasively quantify CBF without injection or exposure to ionizing radiation (7–11, 34, 35). While there is better spatial resolution compared with nuclear medicine studies, there has been no standardized approach to quantification of ASL by MRI, segmentation of GM/WM, or a uniform approach to delineation of vascular territories. Of the few studies that have looked at ASL perfusion in children with SCA, the majority have confirmed the known elevated CBF in the untreated population (7–9), compared with known normal controls values, although the absolute values varied depending on the value assigned for the T1 of blood, and GM/WM segmentation techniques. Elevated whole brain mean GM CBF ranged from 112 ± 36 mL/min/100 g (8) to 152.8 ± 42.5 mL/min/100 g (7). In contrast, in our previous study we found near normal whole brain GM CBF (87 ± 24 mL/min/100 g) (11). However, the majority (18/21) of the patients we evaluated had been treated on hydroxyurea for a median of 4.5 years. Our patients had less severe anemia, increased fetal hemoglobin, normal white blood cell count, and lower MCA transcranial doppler (TCD) velocities consistent with the therapeutic effects of hydroxyurea. Zimmerman, et al. also reported lower TCD velocities in hydroxyurea treated patients, which suggests that treatment with hydroxyurea helps to normalize CBF (36). One recent ASL study of untreated children with SCA performed at 3T found no difference in resting CBF in patients with SCA and controls (10).

In previous studies of CBF by ASL in children with SCA that included GM and WM segmentation, the delineation of tissue type and vascular territories was performed on the ASL images hand drawn based on Tatu's accepted vascular atlas (7, 8, 10, 11, 17). We employed an established automated segmentation (20) of conventional MRI images to more precisely delineate GM from WM. Despite the advantage of automated segmentation, manual delineation of the major vascular territories still required significant time. Given that elevated CBF is associated with increased stroke risk (14), impaired adaptive response to passive visual stimuli (13), lower performance intelligence quotients (8) and possible correlation with hematological variables (14), there is a need for standardized and efficient ways to delineate cerebral vascular territories for regional evaluation of CBF and other imaging parameters in prospective clinical trials and research protocols.

Previous studies have found developmental and gender difference in CBF. Normal cerebral blood flow peaks in the early years of life, and then declines quickly between teenagers and adults (37). Pertinent to this manuscript, Biagi found that CBF values were 97 ± 5/26 ± 1 mL/min/100 g in GM/WM of children (mean age 7± 3 years), and 79 ± 3/22 ± 1 mL/min/100 g in teenagers (16 ± 2years). We found no effect of age on CBF, likely in part the result of our relatively small sample size. Likewise, CBF is generally reported to be higher in females than males at any given age (38–40), For example, Parkes discovered the mean CBF by ASL of males (M) vs. females (F) to be GM: M 58 ±13 mL/min/100 g vs. F 68 ± 10 mL/min/100 g, WM: M 23 ±3 mL/min/100 g vs. F 25 ± 5 mL/min/100 g in her

cohort, [M mean age 44(SD 12), F mean age 39(SD 15)] (38). We found no significant gender CBF in our SCA cohort, which may reflect our small sample size and skewed male to female ratio.

We found significant associations between CBF and the absolute reticulocyte count, hemoglobin and hemoglobin F. In our previous report (11), we analyzed all available hematological data and found no relationship with CBF. In this analysis with the semi-automated approach, we limited the interval between imaging and clinical laboratory evaluations to a maximum of 4 weeks (most within one week). This analysis detected significant associations between CBF and hematological variables of interest. We found a positive correlation between the degree of hemolysis as indicated by the continuous variable absolute reticulocyte count and increasing CBF in multiple WM regions and negative correlation with hemoglobin and hemoglobin F in the bilateral PCA WM and right PCA WM respectively. Additionally, there was a trend toward significance with hemoglobin F in the left PCA WM as well. Indeed, the amount of fetal hemoglobin expression is associated with a milder clinical phenotype of the disease, and is an area of active research (41, 42). These significant hematological associations are clinically relevant relationships, and may in part demonstrate complex pathophysiologic changes that contribute to observed clinical variation in CBF (14), although this needs to be validated in a prospective study.

There are several practical advantages of semi-automated delineation of vascular territories compared to the manual approach. The semi-automated method is very quick from a human time perspective and offers a reasonable alternative to manual delineation. The semi-automated is less operator dependent, which reduces a source of variation and potential bias. More standardized and rapid division of brain parenchyma into vascular territories facilitates broader application of vascular territory based CBF evaluation.

Several limitations of this study should be noted. While the semi-automated method is less operator dependent, there is still room for operator error because it is not fully automated. The CBF measurements were limited by ASL brain coverage in this study, which was from an older protocol. While we realize that there is considerable individual variability in normal patients, we did not have vessel selective coils to image each individual territory. The vascular territories were defined as strictly conventional vascular regions based on accepted atlases and the relation of these regions to various anatomic landmarks, not necessarily correlating perfectly to a physiologic territory. Nevertheless, the territories represent conventionally accepted regions in a standardized fashion, and they yielded equivalent measurements of CBF. Lastly, the small sample size may have limited statistical power of possible correlation between age, gender and CBF.

In conclusion, our study demonstrated that the SA method for CBF delineation of vascular territories provided a valid and faster tool to facilitate standardized evaluation of CBF in children with SCA. Demonstrated associations between CBF and hematologic variables may reflect pathophysiologic changes that contribute to clinical variation in CBF.

Acknowledgments

This work was supported in part by Comprehensive Sickle Cell Center grant U54HL70590 from the National Heart, Lung, and Blood Institute, the Cancer Center Support (CORE) grant P30CA21765 from the National Cancer Institute, and by the American Lebanese Syrian Associated Charities (ALSAC).

The authors would like to acknowledge Zoltan Patay, MD, PhD for his thoughtful review of this manuscript.

References

1. Sheth S, Licursi M, Bhatia M. Sickle cell disease: time for a closer look at treatment options? British journal of haematology. 2013; 162(4):455–464. [PubMed: 23772687]
2. Moser FG, Miller ST, Bello JA, et al. The spectrum of brain MR abnormalities in sickle-cell disease: a report from the Cooperative Study of Sickle Cell Disease. AJNR American journal of neuroradiology. 1996; 17(5):965–972. [PubMed: 8733975]
3. Steen RG, Emudianughe T, Hankins GM, et al. Brain imaging findings in pediatric patients with sickle cell disease. Radiology. 2003; 228(1):216–225. [PubMed: 12775848]
4. Platt OS, Brambilla DJ, Rosse WF, et al. Mortality in sickle cell disease. Life expectancy and risk factors for early death. The New England journal of medicine. 1994; 330(23):1639–1644. [PubMed: 7993409]
5. Lanzkron S, Carroll CP, Haywood C Jr. Mortality rates and age at death from sickle cell disease: U.S. 1979–2005. Public Health Rep. 2013; 128(2):110–116. [PubMed: 23450875]
6. Vichinsky EP, Neumayr LD, Gold JI, et al. Neuropsychological dysfunction and neuroimaging abnormalities in neurologically intact adults with sickle cell anemia. JAMA. 2010; 303(18):1823–1831. [PubMed: 20460621]
7. Oguz KK, Golay X, Pizzini FB, et al. Sickle cell disease: continuous arterial spin-labeling perfusion MR imaging in children. Radiology. 2003; 227(2):567–574. [PubMed: 12663827]
8. Strouse JJ, Cox CS, Melhem ER, et al. Inverse correlation between cerebral blood flow measured by continuous arterial spin-labeling (CASL) MRI and neurocognitive function in children with sickle cell anemia (SCA). Blood. 2006; 108(1):379–381. [PubMed: 16537809]
9. Gevers S, Nederveen AJ, Fijnvandraat K, et al. Arterial spin labeling measurement of cerebral perfusion in children with sickle cell disease. J Magn Reson Imaging. 2012; 35(4):779–787. [PubMed: 22095695]
10. van den Tweel XW, Nederveen AJ, Majoie CB, et al. Cerebral blood flow measurement in children with sickle cell disease using continuous arterial spin labeling at 3. 0-Tesla. MRI Stroke; a journal of cerebral circulation. 2009; 40(3):795–800.
11. Helton KJ, Paydar A, Glass J, et al. Arterial spin-labeled perfusion combined with segmentation techniques to evaluate cerebral blood flow in white and gray matter of children with sickle cell anemia. Pediatric blood & cancer. 2009; 52(1):85–91. [PubMed: 18937311]
12. Prohovnik I, Pavlakis SG, Piomelli S, et al. Cerebral hyperemia, stroke, and transfusion in sickle cell disease. Neurology. 1989; 39(3):344–348. [PubMed: 2927641]
13. Zou P, Helton KJ, Smeltzer M, et al. Hemodynamic responses to visual stimulation in children with sickle cell anemia. Brain imaging and behavior. 2011; 5(4):295–306. [PubMed: 21881848]
14. Prohovnik I, Hurlet-Jensen A, Adams R, De Vivo D, Pavlakis SG. Hemodynamic etiology of elevated flow velocity and stroke in sickle-cell disease. Journal of cerebral blood flow and metabolism: official journal of the International Society of Cerebral Blood Flow and Metabolism. 2009; 29(4):803–810.
15. Kirkham FJ, Datta AK. Hypoxic adaptation during development: relation to pattern of neurological presentation and cognitive disability. Developmental science. 2006; 9(4):411–427. [PubMed: 16764614]
16. Luh WM, Wong EC, Bandettini PA, Hyde JS. QUIPSS II with thin-slice TI1 periodic saturation: a method for improving accuracy of quantitative perfusion imaging using pulsed arterial spin labeling. Magnetic resonance in medicine: official journal of the Society of Magnetic Resonance in Medicine/Society of Magnetic Resonance in Medicine. 1999; 41(6):1246–1254.

17. Tatu L, Moulin T, Bogousslavsky J, Duvernoy H. Arterial territories of the human brain: cerebral hemispheres. Neurology. 1998; 50(6):1699–1708. [PubMed: 9633714]
18. Ji Q, Glass JO, Reddick WE. A novel, fast entropy-minimization algorithm for bias field correction in MR images. Magnetic resonance imaging. 2007; 25(2):259–264. [PubMed: 17275623]
19. Reddick WE, Glass JO, Cook EN, Elkin TD, Deaton RJ. Automated segmentation and classification of multispectral magnetic resonance images of brain using artificial neural networks. IEEE transactions on medical imaging. 1997; 16(6):911–918. [PubMed: 9533591]
20. Glass JO, Reddick WE, Reeves C, Pui CH. Improving the segmentation of therapy-induced leukoencephalopathy in children with acute lymphoblastic leukemia using a priori information and a gradient magnitude threshold. Magnetic resonance in medicine: official journal of the Society of Magnetic Resonance in Medicine/Society of Magnetic Resonance in Medicine. 2004; 52(6):1336–1341.
21. Kretschmann, HJ.; Weinrich, W. Cranial Neuroimaging and Clinical Neuroanatomy: Atlas of MR Imaging and COmputed Tomography. Stuttgart, Germany: Thieme; 2004.
22. Woolsey, TA.; Hanaway, J.; Gado, MH. The Brain Atlas, A Visual Guide to the Human Central Nervous System. Hoboken, New Jersey: Wiley & Sons, Inc; 2003.
23. Osborn, AG. Diagnostic Neuroradiology. St. Louis: Mosby; 1994. p. 130-131.
24. Savoiardo M. The vascular territories of the carotid and vertebrobasilar systems. Diagrams based on CT studies of infarcts Italian journal of neurological sciences. 1986; 7(4):405–409. [PubMed: 3759413]
25. Smithuis, R. Brain Ischemia - Vascular territories. In: Smithuis, R.; van Delden, O., editors. Radiology Assistant: Radiological Society of the Netherlands. 2008.
26. Vichinsky EP, Neumayr LD, Earles AN, et al. Causes and outcomes of the acute chest syndrome in sickle cell disease. National Acute Chest Syndrome Study Group. The New England journal of medicine. 2000; 342(25):1855–1865. [PubMed: 10861320]
27. Hollander, M.; Wolfe, DA. Nonparametric Statistical Methods. John Wiley & Sons; 1999. p. 787
28. Altman DG, Bland JM. Measurement in Medicine: the Analysis of method Comparison Studies. Journal of the Royal Statistical Society Series D (The Statistician). 1983; 32(3):307–317.
29. Landis JR, Koch GG. The measurement of observer agreement for categorical data. Biometrics. 1977; 33(1):159–174. [PubMed: 843571]
30. Prengler M, Pavlakis SG, Prohovnik I, Adams RJ. Sickle cell disease: the neurological complications. Annals of neurology. 2002; 51(5):543–552. [PubMed: 12112099]
31. Herold S, Brozovic M, Gibbs J, et al. Measurement of regional cerebral blood flow, blood volume and oxygen metabolism in patients with sickle cell disease using positron emission tomography. Stroke; a journal of cerebral circulation. 1986; 17(4):692–698.
32. Powars DR, Conti PS, Wong WY, et al. Cerebral vasculopathy in sickle cell anemia: diagnostic contribution of positron emission tomography. Blood. 1999; 93(1):71–79. [PubMed: 9864148]
33. Tzika AA, Massoth RJ, Ball WS Jr, Majumdar S, Dunn RS, Kirks DR. Cerebral perfusion in children: detection with dynamic contrast-enhanced T2*-weighted MR images. Radiology. 1993; 187(2):449–458. [PubMed: 8475289]
34. Wang J, Licht DJ, Jahng GH, et al. Pediatric perfusion imaging using pulsed arterial spin labeling. Journal of magnetic resonance imaging: JMRI. 2003; 18(4):404–413. [PubMed: 14508776]
35. Floyd TF, Ratcliffe SJ, Wang J, Resch B, Detre JA. Precision of the CASL-perfusion MRI technique for the measurement of cerebral blood flow in whole brain and vascular territories. Journal of magnetic resonance imaging: JMRI. 2003; 18(6):649–655. [PubMed: 14635149]
36. Zimmerman SA, Schultz WH, Burgett S, Mortier NA, Ware RE. Hydroxyurea therapy lowers transcranial Doppler flow velocities in children with sickle cell anemia. Blood. 2007; 110(3):1043–1047. [PubMed: 17429008]
37. Biagi L, Abbruzzese A, Bianchi MC, Alsop DC, Del Guerra A, Tosetti M. Age dependence of cerebral perfusion assessed by magnetic resonance continuous arterial spin labeling. Journal of magnetic resonance imaging: JMRI. 2007; 25(4):696–702. [PubMed: 17279531]
38. Parkes LM, Rashid W, Chard DT, Tofts PS. Normal cerebral perfusion measurements using arterial spin labeling: reproducibility, stability, and age and gender effects. Magnetic resonance in

medicine: official journal of the Society of Magnetic Resonance in Medicine/Society of Magnetic Resonance in Medicine. 2004; 51(4):736–743.

39. Podreka I, Baumgartner C, Suess E, et al. Quantification of regional cerebral blood flow with IMP-SPECT. Reproducibility and clinical relevance of flow values. Stroke; a journal of cerebral circulation. 1989; 20(2):183–191.
40. Shaw T, Meyer JS, Mortel K, Curtai M, Sakai F, Yamaguchi F. Effects of normal aging, sex and risk factors for stroke on regional cerebral blood flow (rCBF) in normal volunteers. Acta Neurologica Scandinavica. 1979; (60):462–463.
41. Eridani S, Mosca A. Fetal hemoglobin reactivation and cell engineering in the treatment of sickle cell anemia. Journal of blood medicine. 2011; 2:23–30. [PubMed: 22287860]
42. Dasgupta T, Fabry ME, Kaul DK. Antisickling property of fetal hemoglobin enhances nitric oxide bioavailability and ameliorates organ oxidative stress in transgenic-knockout sickle mice. American journal of physiology Regulatory, integrative and comparative physiology. 2010; 298(2):R394–402.

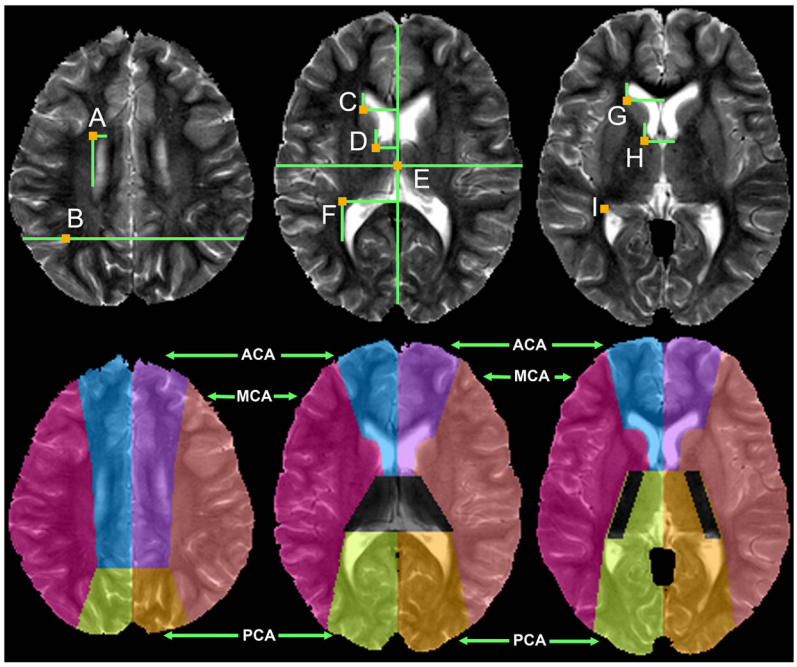

Figure 1.

The semi-automated technique relied on identifying anatomic landmarks on specific sections (top row). *Upper Slice* (the level that the ventricles first appear) - (A) the junction of a vertical line adjacent to the body of the lateral ventricle and a horizontal line from the anterior aspect of the ventricle, (B) the Superior Temporal Sulci; *Middle Slice* (the level of the basal ganglia at the lowest point of the genu of the corpus callosum [CC]) - (C) junction of a horizontal line from the most posterior edge of the genu of the CC and a vertical line from the anterior lateral edge of the frontal horn, (D) junction of a vertical line from lateral edge of the posterior aspect of the frontal horn and a horizontal line from posterior aspect of the frontal horn, (E) center of the image, (F) junction of a horizontal line from the most anterior edge of the splenium of the CC and a vertical line from the lateral edge of the occipital horn; *Lower Slice* (lowest point of the genu of the CC, at the level of the thalamus, first appearance of the cerebellum) - (G) junction of a horizontal line from the most posterior edge of the genu of the CC and vertical line from lateral frontal horn, (H) junction of a vertical line from lateral edge of the posterior aspect of the frontal horn and a horizontal line from posterior aspect of the frontal horn, (I) anterior point at lateral aspect of occipital horn. These landmarks were then used to distinguish the left and right anterior cerebral artery (ACA), middle cerebral artery (MCA), and posterior cerebral artery (PCA) regions (bottom row).

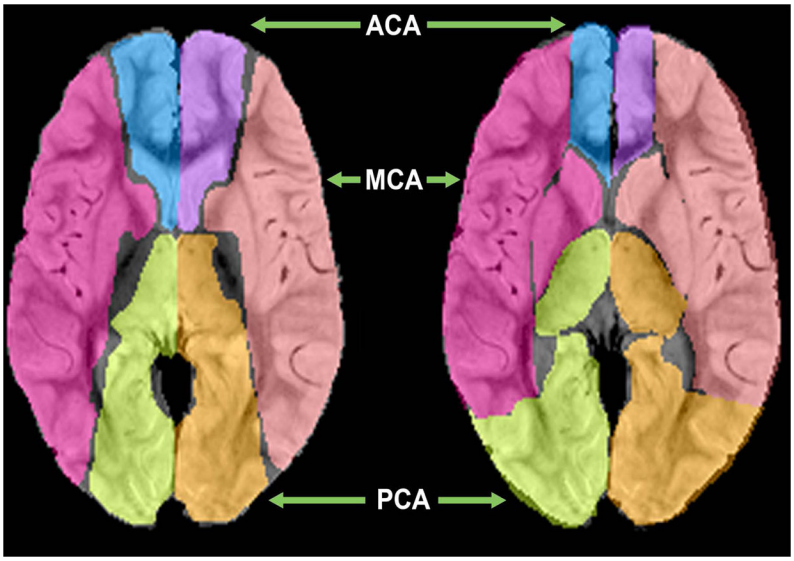

Figure 2.

Visual representation of delineation by semi-automated (left) vs. manual (right) techniques. Notice that the absence of the delineation of the anterior choroidal artery region in the SA method. Despite differences, the Kappa Index showed substantial (ACAs, PCAs) to almost perfect agreement (MCAs) between the pixels selected by both methods.

Figure 3.

Visual representation of the layering process of the segmentation and vascular territory identification applied to the ASL output map. Segmented output (left) shows gray matter in yellow and white matter in green. Vascular territory map (left center) shows the ACA in #, MCA in #, and the PCA in #. An example grayscale CBF map is provided (right center). Limiting this to just the gray and white matter of the MCA is demonstrated on right.

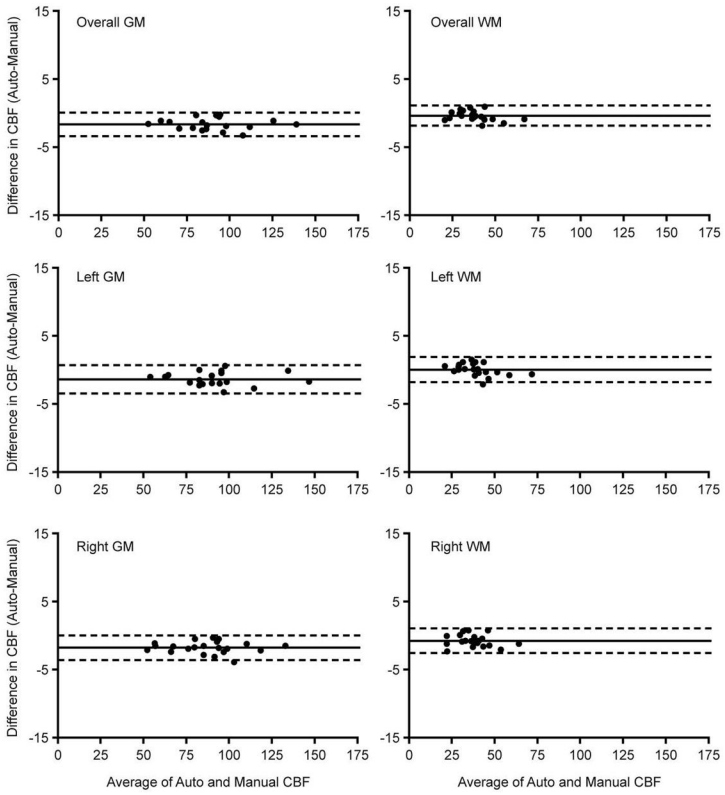

Figure 4.

Bland-Altman plots and limits of agreement demonstrate the level of agreement between the manual delineation versus the semi-automated techniques of the whole brain, left and right hemispheres gray and white matter CBF.

Table 1

Median CBF values (range: min, max) from SA and M techniques within whole brain, hemisphere, and vascular territory.

	Gray Matter		White Matter	
Region	**SA**	**M**	**SA**	**M**
Whole Brain	86 (52, 138)	88 (53, 140)	37 (20, 67)	38 (21, 68)
Left Brain	88 (53, 145)	90 (54, 146)	38 (21, 71)	37 (20, 71)
Right Brain	89 (51, 132)	90 (53, 133)	37 (20, 63)	38 (21, 64)
Left ACA	73 (37, 121)	83 (44, 132)	28 (10, 54)	31 (16, 61)
Left MCA	81 (52, 142)	82 (48, 138)	38 (20, 67)	34 (17, 64)
Left PCA	101 (62, 164)	106 (66, 180)	48 (27, 97)	49 (28, 104)
Right ACA	70 (38, 120)	75 (41, 114)	27 (7, 56)	31 (16, 57)
Right MCA	81 (46, 127)	79 (46, 125)	32 (18, 60)	30 (14, 56)
Right PCA	103 (64, 156)	105 (64, 175)	48 (26, 96)	50 (31, 102)

CBF=cerebral blood flow, ACA=anterior cerebral artery, MCA=middle cerebral artery, PCA=posterior cerebral artery. CBF is reported as mL/100g/min, SA = Semi-Automated, M=Manual.

Table 2

Pearson Correlation Coefficients between regional CBF measurements based on manual and semi-automated delineation of vascular territories.

	Gray Matter		White Matter	
	Whole Brain 0.99		Whole Brain 0.99	
	Left	Right	Left	Right
Brain	0.99	0.99	0.99	0.99
ACA	0.96	0.98	0.93	0.94
MCA	0.99	0.99	0.98	0.98
PCA	0.97	0.96	0.91	0.89

All p-values < .0001, CBF=cerebral blood flow, ACA=anterior cerebral artery, MCA=middle cerebral artery, PCA=posterior cerebral artery

Table 3

Correlations between CBF in semi-automatically delineated vascular territories and hematologic variables

Region	Tissue	Hemoglobin	Hemoglobin F	ARC
		9.7 (6.2 – 11.6)	13.8 (2.1 – 32.6)	0.14 (0.06 – 0.42)
Whole Brain	WM	-	-	0.53 (0.02)
Left Brain	WM	-	-	0.49 (0.03)
Right Brain	WM	-	-	0.56 (0.01)
Left MCA	WM	-	-	*0.41 (0.07)*
Left PCA	WM	−0.48 (0.03)	*−0.42 (0.09)*	0.58 (0.01)
Left PCA	GM	-	-	0.58 (0.01)
Right MCA	WM	-	-	0.50 (0.02)
Right PCA	WM	−0.47 (0.04)	−0.47 (0.049)	0.73 (<0.001)
Right PCA	GM	-	-	0.53 (0.02)

Top line represents median values and ranges of the hematologic variables. (P-values) < 0.05 are considered statistically significant, *italicized* indicates trends, and "-"indicates non-significant differences. CBF=cerebral blood flow, WM=white matter, GM=gray matter, MCA=middle cerebral artery, PCA=posterior cerebral artery, ARC=absolute reticulocyte count. CBF is reported as mL/100g/min, Hemoglobin is reported as g/dL and Hemoglobin F as a percentage of the total Hemoglobin, ARC is reported as number of cells × 10^6. No significant correlation was found between any of the CBF measurements and white blood cell count or lifetime acute chest syndrome episodes.

Table 4

Hematological and clinical variables. The values of the hematological variables reflect prior treatment by Hydroxyurea in the majority of the subjects.

Variable	N	Mean	Std Dev	Median	Minimum	Maximum
Hb	20	9.3	1.5	9.7	6.2	11.6
HbF	18	16.2	9.4	13.8	2.1	32.6
ARC	20	0.16	0.09	0.14	0.06	0.42
WBC	20	8.7	3.6	7.6	3.3	15.5
Lifetime_ACS	21	1.8	1.3	2.0	0.0	4.0

Hb=hemoglobin, HbF= hemoglobin F, ARC= absolute reticulocyte count, WBC= white blood cell count, ACS= acute chest syndrome